Accepted Manuscript

Novel synthesis process of methyl ammonium bromide and effect of particle size on structural, optical and thermodynamic behavior of $CH_3NH_3PbBr_3$ organometallic perovskite light harvester

Rajan Kumar Singh, Ranveer Kumar, Amit Kumar, Neha Jain, Rajiv Kr. Singh, Jai Singh

PII: S0925-8388(18)30373-6

DOI: 10.1016/j.jallcom.2018.01.355

Reference: JALCOM 44819

To appear in: *Journal of Alloys and Compounds*

Received Date: 29 August 2017

Revised Date: 12 January 2018

Accepted Date: 27 January 2018

Please cite this article as: R.K. Singh, R. Kumar, A. Kumar, N. Jain, R.K. Singh, J. Singh, Novel synthesis process of methyl ammonium bromide and effect of particle size on structural, optical and thermodynamic behavior of $CH_3NH_3PbBr_3$ organometallic perovskite light harvester, *Journal of Alloys and Compounds* (2018), doi: 10.1016/j.jallcom.2018.01.355.

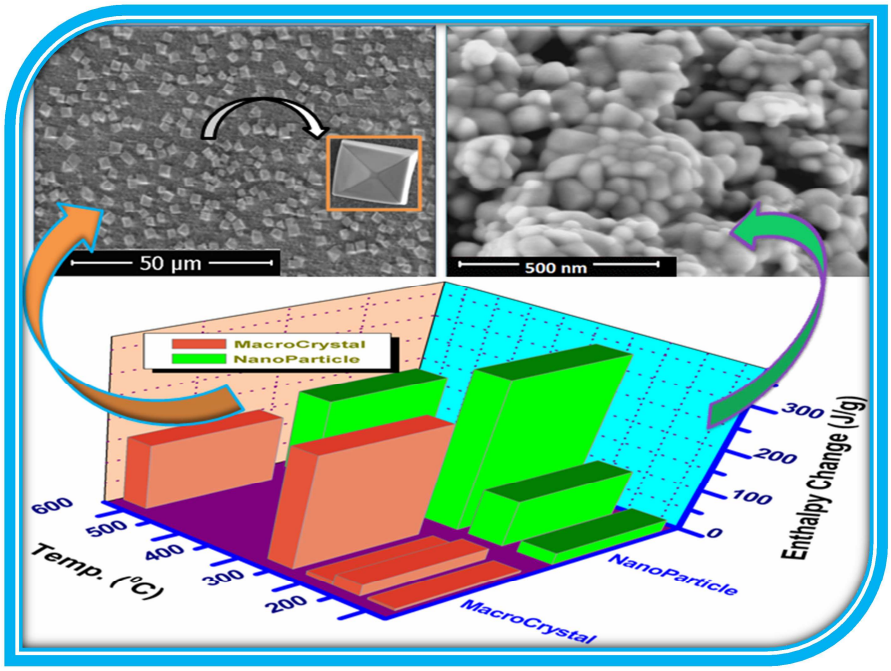

Novel synthesis process of methyl ammonium bromide and effect of particle size on structural, optical and thermodynamic behavior of $CH_3NH_3PbBr_3$ organometallic perovskite light harvester

Rajan Kumar Singh[1], Ranveer Kumar[1*],Amit Kumar[2], Neha Jain[1], Rajiv Kr. Singh[2], and Jai Singh[1]

[1]Department of Physics, Dr. Harisingh Gour Central University, Sagar – 470003, M. P. India

[2]Advanced Material & Devices Division, CSIR, National Physical Laboratory, New Delhi – India

* *Corresponding author:ranveerssi@yahoo.com*

Abstract:

A simple, cost effective production approach having high stability is pertinent to any organic-inorganic perovskite solar cells. The main focus of the present work has been to formulate and estimate the stability of $CH_3NH_3PbBr_3$ micro-cubes and nanoparticles based perovskite solar cells. Firstly, novel synthesis route has been introduced for the preparation of CH_3NH_3Br (MABr) electrolyte salt which is less time consuming, as well as cost effective than pristine methods. We also reported a facile single solution process to grow large scale $CH_3NH_3PbBr_3$ ($MAPbBr_3$) hybrid perovskite micro-cubes and nano-particles. The effect of different size (micro-cube & nano-particles) of perovskite material on structural, optical, thermal stability and degradation kinetics has been examined. X-ray diffraction spectra of $MAPbBr_3$ perovskite reflect high crystallinity and cubic structure of the material at the room temperature. The surface morphology of micro-cubes and nano-particle $MAPbBr_3$ has been obtained from scanning electron microscope (SEM). Broad absorption spectrum has found in the visible region with high absorption coefficient and PL spectra show the green emission which is in good agreement with the optical band gap of $MAPbBr_3$ from absorption measurements. With decreasing the size of perovskite materials, band gap and emission spectra tuned towards the blue region. The simultaneous thermal analysis (STA) study indicates towards the more thermal stability of micro-cubes structures than nanoparticles material while the change in enthalpy (ΔH) and specific heat capacity (ΔCp) of nano particle have increased by reducing the particle size of perovskite due to modification of endothermic peaks.

Keywords: Perovskite, Chemical Synthesis, Microstructure, Nanostructure, Optical Properties, Enthalp

Graphical Abstract:

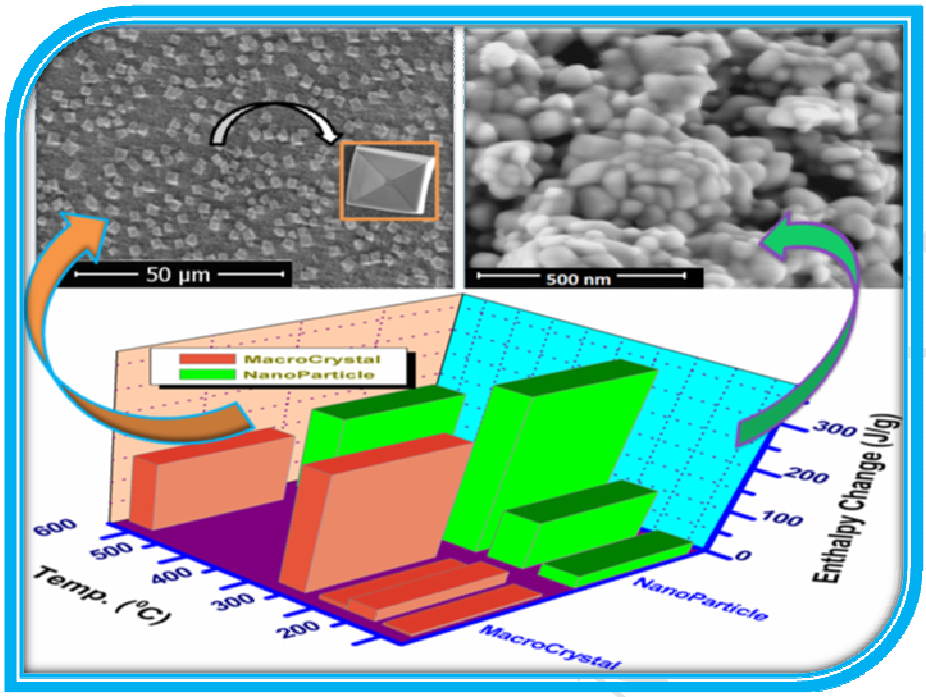

Highlights:

- Solution processed methyl ammonium lead bromide was highly cubic crystalline at room temperature.
- $MAPbBr_3$, micro-cubes was more thermally stable than nano-particles.
- High absorbance and luminescence property show the light harvesting nature of the materials.
- Change in enthalpy and specific heat capacity of perovskite particle was increased by reducing the particle size.

1. Introduction

Recent development in nanoscience and nanotechnology has not only brought potential building block for nanoelectronics, optoelectronics, but also offer a breakthrough in photovoltaic performance in devices[1, 2].Hybrid perovskites have attracted attention in recent years due to their excellent potential as light harvesting material for application in solar cells and light emitting diodes[3,4]. Furthermore, the extraordinary properties of color tunability/optical absorption, high absorption coefficient, excellentphotoluminescence efficiency and low non-radiative recombination rates, extends their applications into various optoelectronic devices such as solar cell, light emitting diodes, photo detectors, light emitting cables and optical memory etc[5-9].

In 2009 Miyasaka group have used OIHP absorber layer for photovoltaic devices first time with 3.8% power conversion efficiency (PCE)[10]. After this discovery many groups have fabricated different types of OIHP materials tuning with the A, B and X sites of the perovskite materials[11-15]. Recently, national renewable energy laboratory (NREL) has certified the maximum 22.7% PCE of the perovskite solar cell[16]. Weber et al. successfully studied the various composition of the 3-dimensional (3-D) $CH_3NH_3PbX_3$ perovskite material by tuning their crystal structure and phases[17,18]. They have reported that $MAPbBr_3$ ($MA=CH_3NH_3$) perovskite material shows the cubic phase I (Pm3m), tetragonal phase II (I4mcm) and orthorhombic phase IV (Pnma, z = 4) for different temperature.OIHP compounds have wide direct band gap and this direct band gap of the materials can be tuned by either changing the Agroup,B group or the X group. $MAPbBr_3$ material is a p-type semiconductor with a direct band gap of 1.93-2.3eV that corresponds to an absorption onset of ≤550nm[19,20]. This excellent optical property of the material stands it in the first row of the light harvesting materials. Optical properties of perovskite material very interestingly changes with particle size of the material. Effect of particle size recently have been reported, with reducing size of particle, blue shifting in absorption edge and increase in photoluminescence obtained[5,6]. Gao et al has synthesized $CH_3NH_3PbBr_3$ perovskite of the micro-plates and micro-rods. They have studied the three-photon process in single crystal

$CH_3NH_3PbBr_3$ microstructures[9]. They have observed a three-photon excited whispering-gallery-mode laser experimentally in both of perovskite micro-plate and micro-rod micro-structures. Wenger et al has been synthesized single crystals of methylammonium lead bromide ($CH_3NH_3PbBr_3$) using the rapid growth route[5]. The as synthesized material has been characterised via optical absorption and photoluminescence and show that the optical properties have found almost the same to that of polycrystalline $CH_3NH_3PbBr_3$ films.

Additionally, absorption coefficients of the OIHP materials are greater than traditional semiconducting materials such as silicon, gallium arsenide, N719 conventional dye molecules etc[21]. The photoluminescence property of $MAPbBr_3$ perovskite material is of great interest due to its emissive property. Perez-Prieo group first achieved this type of perovskite nanoparticles with a bright photoluminescence (PL) peak at around 530nm wavelength[22]. Thermal properties of different hybrid perovskite materials containing pure halide and mixed halide have been reported by different research groups[23]. Liu et al. reported that by changing the halide composition of perovskite materials, thermal stability of materials changes due to different decomposition behavior of precursors. Mixed halide perovskites are more thermally stable than pure halide compounds. That's why for thin filmpreparation, mixed halide perovskite films are required slightly higher temperature and more time[24]. In our recent work, we also found that, precursor ratio of the compound play an important roal for thermal stability and crystallization[25]. For pure halide perovskite equal molar ratio was found perfect but in case of mixed halide, precursor ratio can be tuned by suitable stability and capability of structure of the materials. As revealed from the above literature, elaborative work has been carried out on the effect on thermal behavior of different synthesis rout, precursor ratio and halide effect on perovskite materials but joint studies on the effect of particle size on the thermal and optical properties have not been fully available.

Here, we have synthesized the MABr and $MAPbBr_3$ micro-cubes and nano-particles by low cost, solution method without using any legends, additives or purifying agents. We have also investigated the thermal behavior of micro-cubes and nano-particles of prepared perovskite material in ambient conditions.

To prove, $MAPbBr_3$ as a light harvesting material, we have studied the UV-Visible absorption and photoluminescence study with the help of different spectroscopy techniques.Recently,optical and electrical properties of quantum dots, nano-particles and crystalline $MAPbBr_3$ perovskite material have been reported buttheir thermalbehavior is still not reported[26]. The investigation of the effect of particle size of hybrid perovskite on optical and thermal properties will helps to tuning of band gap and thermodynamics behavior of the material.

2. Experimental Section

2.1 Chemicals

Methylamine (40% in methanol, Sigma Aldrich, USA), hydrobromic acid (53% in water) (Merck, India), Lead bromide ($PbBr_2$) (99.99% Sigma Aldrich, USA), N, N'- dimethyleformamide (DMF) (99.8% Sigma Aldrich, USA).

2.2 Synthesis of $MAPbBr_3$

For the preparation of CH_3NH_3Br, methylamine and hydrobromic acid are mixed into 250ml of three necked round bottom flask with continuous stirring at 0°C for 2hrs, homogeneous transparent CH_3NH_3Br solution obtained. CH_3NH_3Br solution isevaporated at 60°C in vacuum oven for 24hrs. White precipitate is obtained after 24hrs vacuum heating and this is grinded with agate mortar pestle and stored in the dry place. The schematic representation of synthesis process is shown in Fig. (S1).In this synthesis rout, there is no need of purification with diethyl ether for long time. Diethyl ether is a hazarded chemical and rapidly vaporized at room temperature. This is used for the purification of electrolyte salt if yellowish MABr is obtained. But in our care, we obtained white and crystalline salt. Therefore there is no need of further purification of material.

For the synthesis of $MAPbBr_3$, prepared MABr and commercial $PbBr_2$ powder are mixed with 1:1 molar ratio in DMF organic solvent. After continuous stirring at 60°C over night, transparent solution is

obtained. This perovskite precursor can be stored for thin film study in glove box. To obtain powder form of perovskite material, precursor is evaporated at 120°C for half an hour in the ambient condition in the Petri dish which gives the cubic orange crystals. To obtain the nano-particle of$MAPbBr_3$, large cubic perovskite crystalshavebeen grinded with agate mortar pestle for 30minutesand store in glove box or vacuum desiccators.

For micro-cube characterization, thin film formed on indium doped tin oxide (ITO) glass substrate. Before the thin perovskite thin film fabrication, ITO glass substrate was sonicated with DI water for 15 minutes and cleaned with soap solution. After soap solution cleaning, substrate was again sonicated with DI water for 15minutes and cleans with acetone & isopropenol treatment respectively. Then prepared, $MAPbBr_3$ perovskite precursor was spin coated on the substrate at a rotation speed of 3000rpm for 30seconds and a uniformed orange film was obtained by annealing at 100˚C for 10minutes.Synthesis Process of $MAPbBr_3$, micro-particles and nano-particles are summarized below:

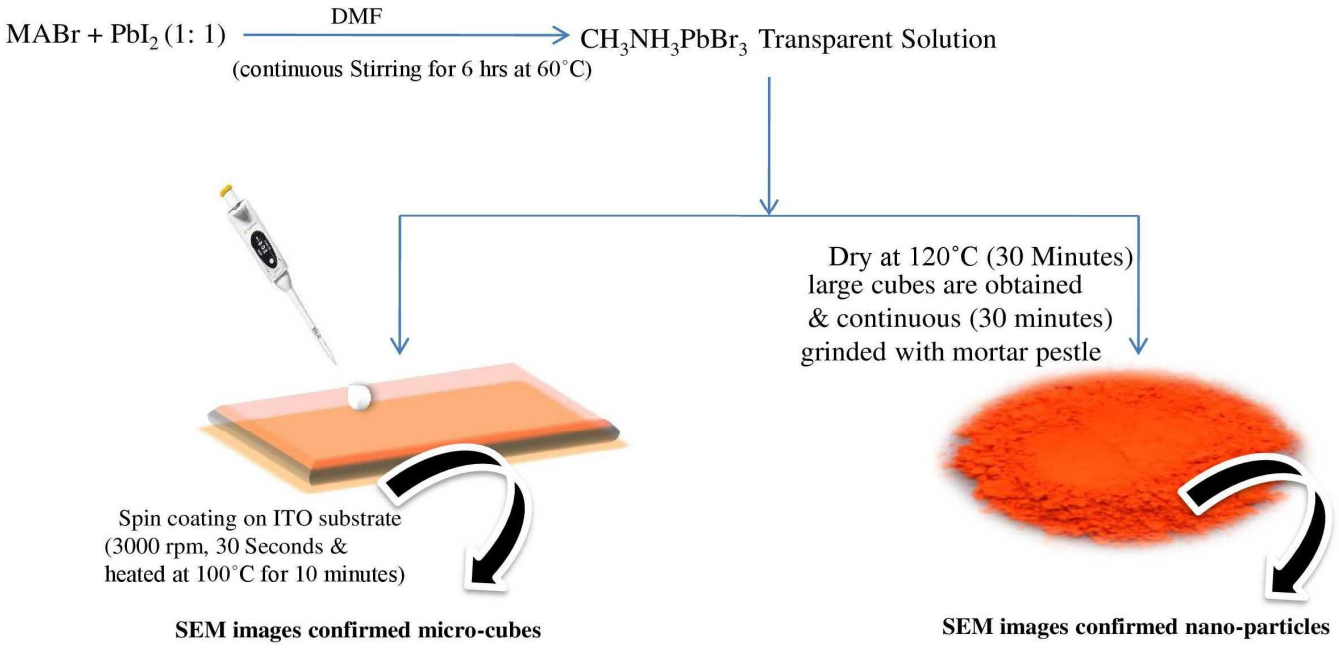

2.3 Characterizations:

Crystal structure was examined by Bruker, Model D8 Discover X-ray Diffractometer using a Cu X-ray tube at voltage of 35kV and 35mA with a step size of 0.02 in ambient conditions.Crystalline phase was

also confirmed by high resolution transmission electron microscope (HRTEM) [*TEMTECNAI G2*] and by corresponding selected area electron beam diffraction. Micrograph of materials was captured by scanning electron microscope *FESEM, Model- Quanta 200 FEI.* Ultraviolet- visible (UV-Vis) absorption and photoluminescence spectrum was measured by UV-2401PC UV-Visrecording spectrometer and photoluminescence spectrometer respectively.For thermal behavior analysis (TG/DTG, DSC), simultaneous thermal analyzer (*NETZCH STA 449 F1 Jupiter*)was used. The samples were heated from room temperature to 700˚C with at a constant rate of 10˚C/min under a nitrogen flow of 60ml/min.

3. Results and Discussion:

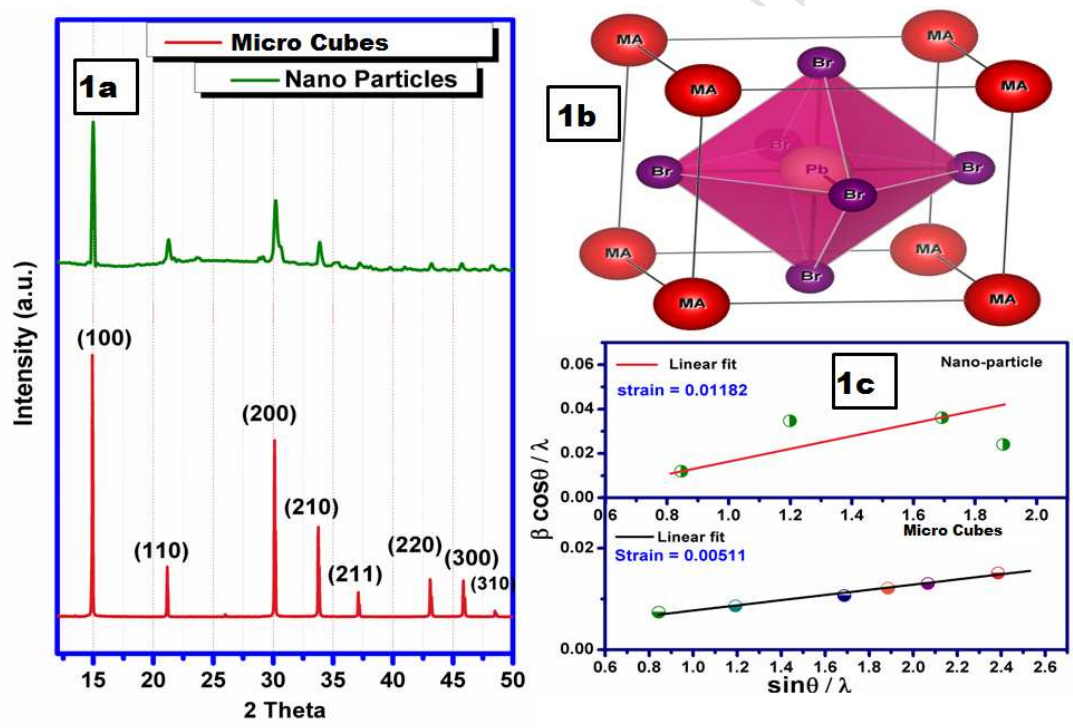

Fig.(1a) XRD patterns of MAPbBr3 micro-cubes and nano-particles respectively, (1b) typical cubic crystal structure of $MAPbBr_3$ by VesTA- software and (1c) Plot for sinθ/λ Vs β cosθ/λ of $MAPbBr_3$ micro cubes and nano-particles

Figure 1(a) shows the X-ray diffraction pattern of the $MAPbBr_3$ nano-particles and micro-cubes in the ambient conditions, which indicate the cubic phase of the perovskite material[22]. The typical peaks at 2θ with

14.95, 21.1, 30.07, 33.69, 37.13, 43.03, 45.91 and 48.55 corresponding to (100), (110), (111), (200), (211), (220), (300), (310), (222), (320) and (321) planes, which indicate the cubic phase of the perovskite material[27]. In addition sharp XRD peaks also demonstrate the phase purity of the cubic $MAPbBr_3$ perovskite structure and with reducing the particle size of perovskite material, broadness of XRD peaks increases and intensity decreases. The polyhedral representation of cubic $MAPbBr_3$ is illustrated by VesTA software as shown in figure 1(b).

From crystal structure, it can be observed that each MA (CH_3NH_3) ion is present on corner of crystal and Pb is present on center of crystal unit. Each bromine is bonded to Pb ion and present on surface of cube. The change in particle size causes change in alignment which affects strain into crystal. In present report, strain is calculated by Williamson Hall plot[28]. The equation from which strain is calculated is

$$\frac{\beta \cos\theta}{\lambda} = \frac{1}{D} + \varepsilon \frac{\sin\theta}{\lambda}$$

Where, θ is Bragg's diffraction angles, β is FWHM (full width at half maximum), D is the effective crystalline site and ε is the micro-strain.

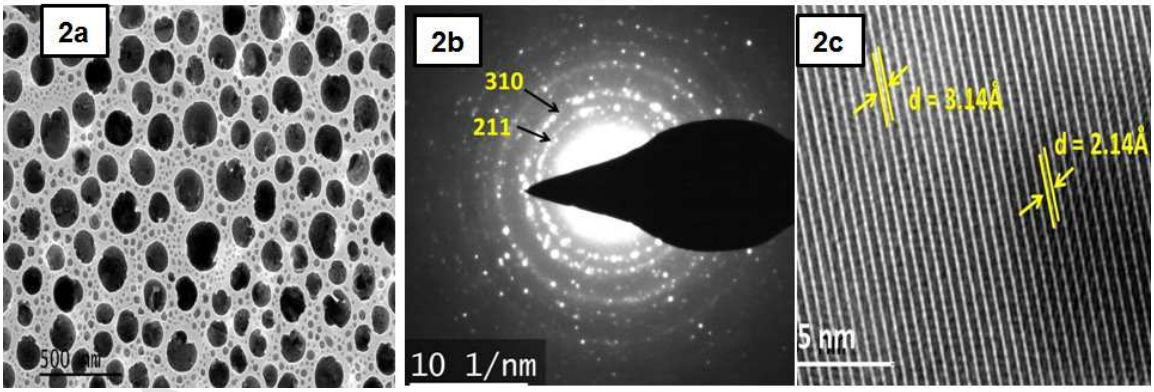

Figure 2: Micrographs of Perovskite materials, (a) TEM image (b) Selected area diffraction pattern and (c) HRTEM image ofnano-particles of the $MAPbBr_3$ Perovskite Material

Figure 1c shows plot between sinθ/λ and β cosθ/λ which estimate micro-strain by slope of graph. It is 0.00511 and 0.01182 for micro and nano-particles. Since micro-strain is increases which decreasing particle

size because of decrease in crystallanity. Fig 2a shows the TEM image of nano-particles of $MAPbBr_3$which was prepared by grinding the micro cubes and deposited on carbon coated copper grid for the TEM analysis.High resolution TEM (HRTEM) image of nano -particle $MAPbBr_3$ hybrid perovskite had shown in fig 2c with lattice fringes spaced by 3.14 and 2.14Å in different regions. This fringe spacing corresponds to the (310) and (211) plane spacing, respectively for the cubic perovskite material. A selected area diffraction patterns (SADP) of the $MAPbBr_3$ (Fig. 2(b) also confirms the (310) and (211) plane present in the perovskite material that indicates the cubic phase of the material at room temperature.

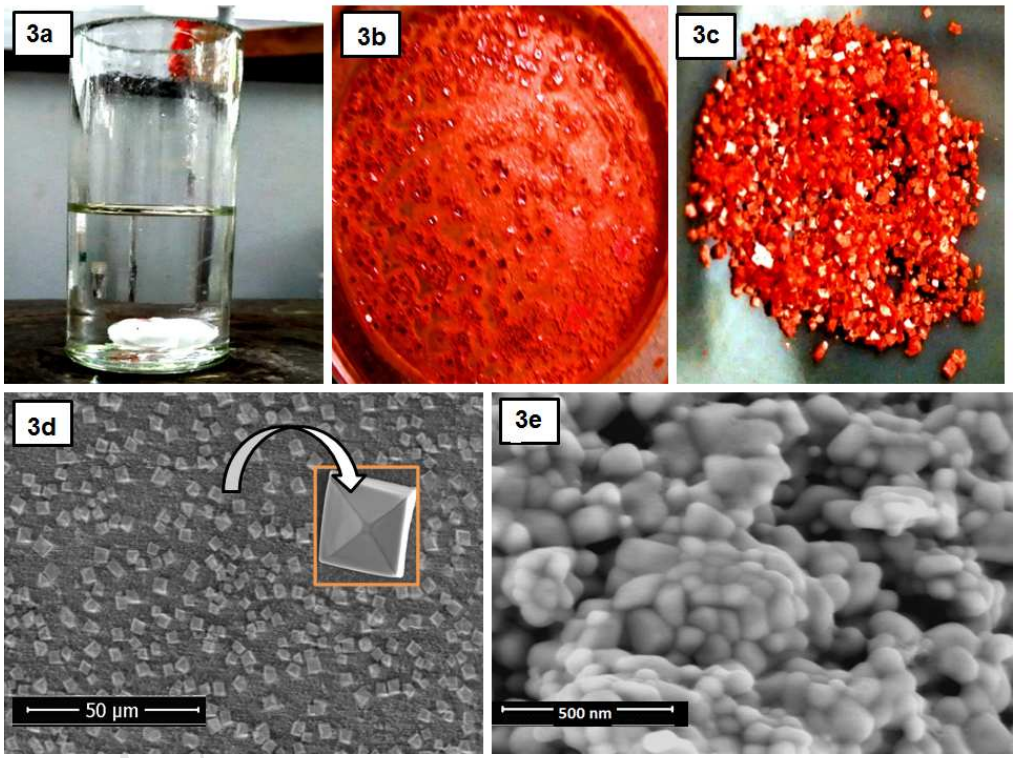

Fig 3,Physical appearance and SEM Micrographs of Perovskite materials, (a) digital image of as prepared perovskite ink (b) digital image of dried $MAPbBr_3$ perovskite at 120˚C (c) digital image of separated cubic crystals from 3b (d) SEM image of cubic crystals (inset figure, single cubic microstructure) &(e) nanoparticles of the $MAPbBr_3$ Perovskite Material

The physical appearance of $MAPbBr_3$ perovskite precursor solution was transparent as shown in fig 3a. In general this perovskite precursor is used for thin film preparation for different device fabrications.

Perovskite precursor was dried at 120˚C which gave orange cubes crystal growth of the material (fig 3b) and these perovskite cubes were separated by sharp twizer (as shown in fig 3c). Further surface morphology of $MAPbBr_3$ had examined by SEM analysis. The SEM images in fig 3(d) and (e) shows the overall morphology of the $MAPbBr_3$ cube crystals and nano-particles. As prepared $MAPbBr_3$ perovskite was large cubes of orange color as shown in digital image in fig 3 b & c and on the other hand when the same precursor solution was deposited on ITO substrate for thin film formation of $MAPbBr_3$, also confirmed the micro cubes like structure (as shown in figure 3d) of the perovskite material[22]. In addition cubic morphology of $MAPbBr_3$ perovskite interestingly converted into spherical particle due to reducing the particle size of the materials which shown in figure 3e and TEM image of fig 2a also confirmed the nano-particle formation of the perovskite materials by grinding of micro cubes.

For the UV - Visible absorption and photoluminescence study, we prepare a thin film of the perovskite material deposited upon ITOsubstrate for bulk perovskite and nanopowder perovskite dispersed in toluene. (Fig. 4) shows the strong and broad absorption spectra is obtained in the visible range between 400 to 700nm which indicates, the light harvesting property of $MAPbBr_3$ perovskite material. Additionally, nanoparticle$MAPbBr_3$ perovskite absorption onset occurs at nearly 521nm, consistent with previous reported works[29, 30].With decreasing the particle size of the same perovskite, absorption onset of UV-visible spectra is shifted towards blue region. The band gap of the material is calculated by using formula, $E_g = 1237.5/\lambda$,where Eg, is band gap of the material and λ is the wavelength of absorption onset curve. The band gap of micro cubes and nano-particles $MAPbBr_3$ is found, 2.15 and 2.22 eV, respectively[31]. Here nanoparticles of perovskite has slightly higher band gap than bulk perovskite because in bulk materials ground state and first excited state levels are very broadened and this broadening leads to narrowing of the band gap. On the other hand broadening in nano materials is less than bulk materials which causes the more energy band gap and blue shift from bulk to nanomaterials[32].

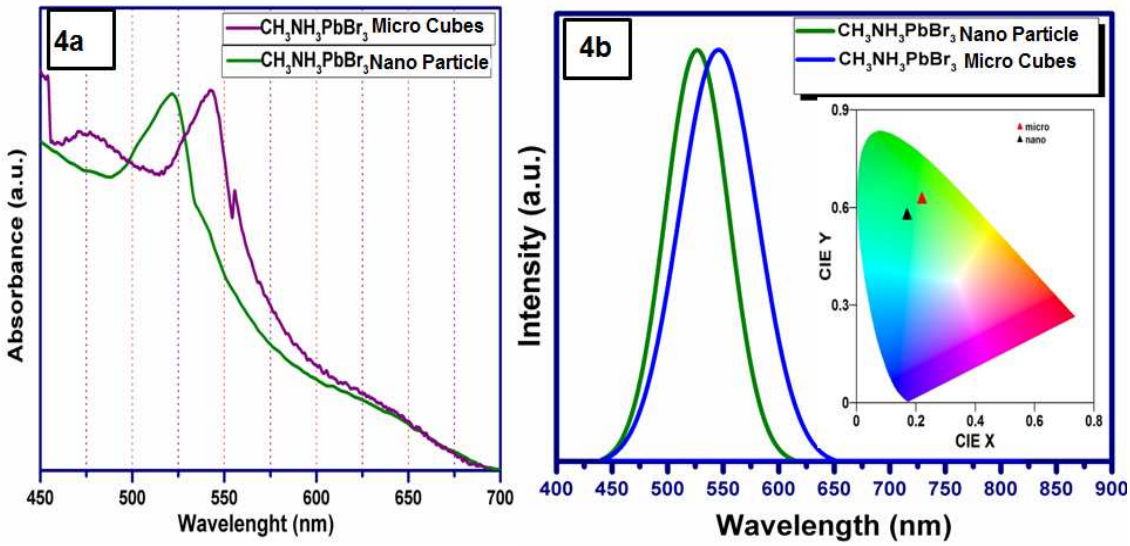

Figure 4:(a) UV-Visible absorption spectraof $MAPbBr_3$micro cubes and nano-particles, (b) Photoluminescence spectra& inset CIE spectrum with 390nm excitation wavelengths of $MAPbBr_3$ micro-cubes and nano-particles.

Figure (4b) shows the photoluminescence (PL) emissionspectra andCIE spectrum of micro cubes and nano-particle of $MAPbBr_3$ perovskite. Similar to UV-Visible onset absorption spectra, PL emission of nanoparticles perovskite indicates blue shift from bulk to nanoparticle which is in good agreement with absorption study of the material. Additionally, CIE spectrum is also confirmed the blue shift with bulk to nanomaterials.From photoluminescence and CIE spectra, it hasalso confirmed that $MAPbBr_3$ material has excellent PL performance and high color purity because no sub spectra or sub-band gap emission is present in PL and CIE spectra[33]. We, we have also found that, the excitation and emission bands of $MAPbBr_3$ organic inorganic halide perovskite offer a larger stokes shift than the typical natural and organic dyes[34, 35].

Thermal stability behavior (TG/DTG) of $MAPbBr_3$ micro cubes and nano particles are shown in figure 5 (a & b). TGA analysis of both particles show, thermal stability of materials up to 200˚C, then it starts losing weight. The extension starting decomposition temperature was determined to be 182°C and the mass loss process ended at around 607°C for micro-particles and 588°C for nano-particles. In 1st step, there

was 18.11% mass loss occurred between 182-300°C due to the decomposition of HBr and next 33.25%mass loss wasoccurred due to decomposition of organic part methylamine up to 400°C. These results also indicate amine group is bounded into the hybrid perovskite matrix more tightly than HBr[23, 36]. But from TGA study of MABr, it is noted that this type of decomposition, by sequential loss of HBr followed by the amine group, has not detected in MABr organic electrolyte salt. MABr was decomposed in one step between 250- 350˚C with sublimation temperature of 250˚C (Fig. S2). this sublimation of mass loss in one step shows the highly purity of MABr. In 3rd stage of mass decomposition 48.13% mass loss occurred between 587-603˚C due to decomposition of $PbBr_2$ within these temperature region (Fig S3).First differential thermogrametry analysis of $MAPbBr_3$, clarify that this perovskite material was decomposed into three steps in which maximum mass loss occurred at 588˚C and minimum mass loss occurred at 278˚C (Fig 5b TGA).

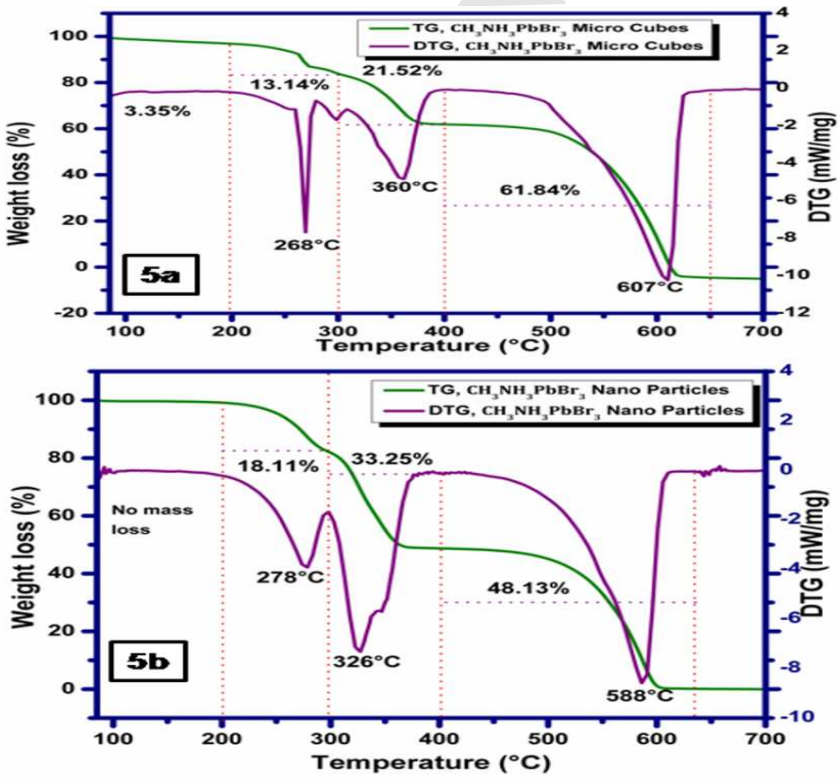

Fig 5 Thermal behavior of TGA (green) and DTG (violet) of (a) $MAPbBr_3$ micro cubes and (b) $MAPbBr_3$ nano-powder

In addition, micro-cubes we have also found that there are differences in thermal stability of $MAPbBr_3$ nanoparticles and cubic crystals. The trend in cubic perovskite crystals was quite similar but the temperature of decomposition and first derivative peaks shifted towards lower values for first degradation step and higher value (360 and 607˚C) for next two decomposition steps suggesting a slightly higher stability of the perovskite micro cubes as shown in fig. (5). From TG/DTG study of both micro and nano-particle of perovskite, it is clear that thermal stability of material also depends on particle size and thermal stability decreases by reducing the particle size of the materials because micro-crystals is formed by bulk amount of materials and it is required more heat for breaking the bonding of materials while in nano-particles there are more surface area available and required less heat to break the bonding in the materials. Thus in both of the cases, perovskite decomposed into three steps which can be understood by given chemical reaction:

$$CH_3NH_3PbBr_3 \leftrightarrow HBr + CH_3NH_2 + PbBr_2$$

Thermal degradation parameters of TG/DTG of both micro cubes and nano particle $MAPbBr_3$ perovskite are summarized in table 1.

Differential scanning Calorimetry (DSC) analysis of the both types of $MAPbBr_3$ perovskites are shown in figure 6 (a and b). The DSC was used to investigate the melting behavior and nature (endothermic/exothermic) of different particle sized perovskite material. DSC graphs show the endothermic nature of both micro and nano particle of perovskites but due to variation of size of $MAPbBr_3$, endothermic peaks are modified. With reducing the particle size, the sharpness and area of endothermic peaks are enhanced. The increased peak area of the endotherm of $MAPbBr_3$ nanoparticle in DSC may be due to the fine size and the greater the rate of diffusion of Nanomaterials. These properties causing the reaction to occur over a much shorter endothermic reactions for the hybrid perovskite materials. Enthalpy change of the micro crystals and nanoparticles of perovskite also have been calculated by DSC analysis (figure 5a and b). Enthalpy change (ΔH) is the amount of heat released or absorbed at constant pressure. Nature of ΔH depends

upon the exothermic and endothermic behavior of the materials. For the endothermic reactions, ΔH is always positive while for exothermic reactions, it is negative[37]. As we discussed above section that different particle size of $MAPbBr_3$ perovskites are endothermic in nature with different peak area.

Table 1: TG/DTG parameters of cubic micro crystals and nano particle of $MAPbBr_3$ perovskite

Materials	**Decomposition Steps**	**Onset & Ended point (˚C)**	**Mass loss in different steps in % (B/wtem.)**			**TGA peaks for diff. steps (˚C)**			**Residual Mass**
			200-300˚C	**300-400˚C**	**400-620˚C**				
Cubic Micro Crystals	3	170 & 607	13.14%	21.52%	61.84%	268	360	607	0.15%
Nano Particle	3	182 & 588	18.11%	33.25%	48.13%	278	326	588	0.51%

ΔH is directly proportional to the peak area of the endothermic reactions. That's why for nano particles perovskite, the value of ΔH is also increased due to increasing the area of endothermic peak. From figure 6, it was concluded that, for larger particle has three small endothermic peaks with ΔH of 5.218, 27.38 & 9.55 J/g up to 300°C while in nanoparticles perovskite two instance endothermic peaks are absorbed with ΔH of 26.62 & 111.3J/g. Additionally two large endothermic peaks were detected near 358 & 610°C (ΔH = 265 & 155.1J/g) in macro size perovskite and in nano particle these peaks are slightly shifted towards lower temperature at 350 & 593°C (ΔH = 349 & 187J/g). Different thermodynamic kinetics (Nature of materials, ΔH and Specific heat capacity i.e. ΔC_p) of DSC of large and nanoparticles perovskite is also

summarizes in table 2. For overall system, enthalpy change for macro particle and Nanomaterials were found 462.25J/g and 574.2J/g respectively.

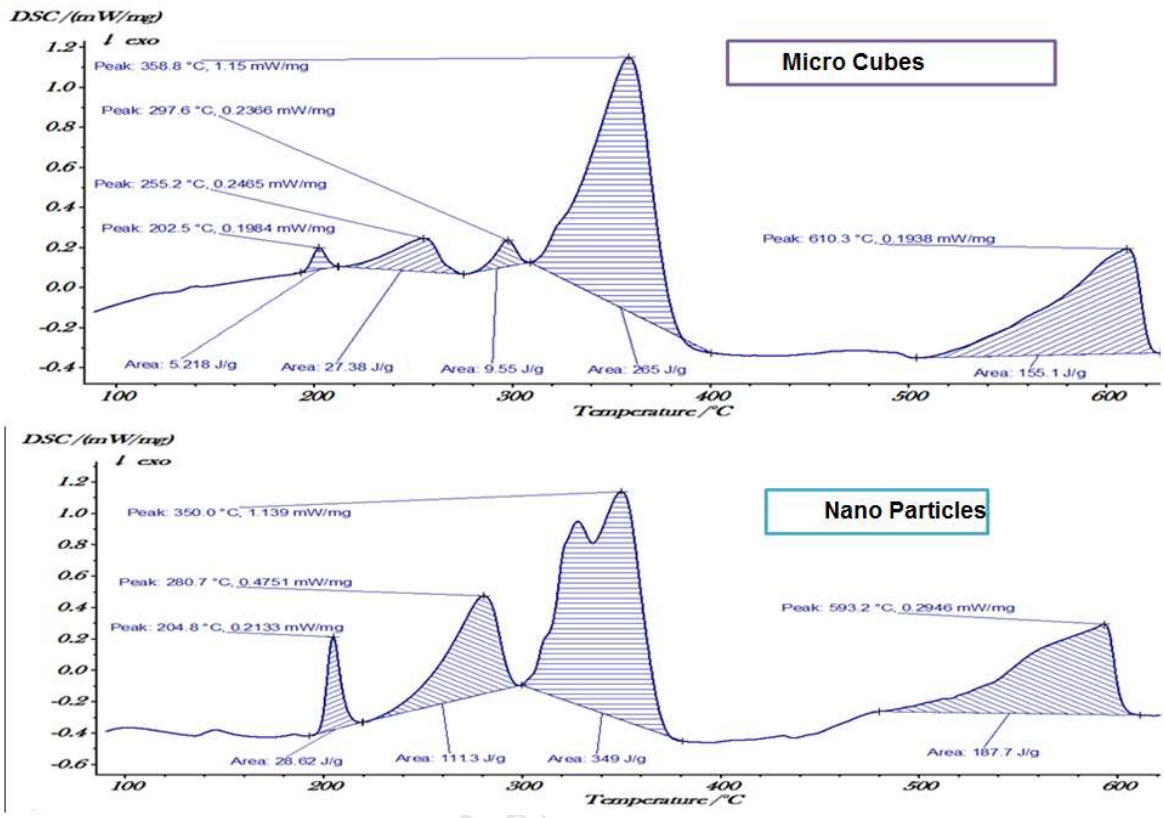

Figure 6: DSC curve with different enthalpy change of (a) micro cubes& (b) nano particle of $MAPbBr_3$

Specific heat capacity (ΔC_p) of the different particle sized perovskite materials were anlysized with the help of DSC curve as given in figure 7 a & b. The specific heat capacity is the amount of heat needed to increase the temperature of one gram of substance by one degree. It can be calculated by $\Delta C_p = \Delta H / \Delta T$, here ΔT is the temperature difference between two endothermic peaks. The heat transfer for different state of matter (solid, liquid & gas) can be stored in various forms of energy such as potential (vibrational mode), translational & rotational kinetic energy. In solid, thermal energy is stored in only vibrational mode and this storage capacity can be measured by calculating ΔC_p. From analysis of ΔC_p of both particles of $MAPbBr_3$, it was concluded that nanoparticles perovskite has mare specific heat capacity compared to the larger perovskite crystals. ΔC_p for different endothermic peaks of the particles also summarized in table 2.

Table 2: DSC kinetics of cubic macro and nanoparticles MAPbBr3 perovskite

$MAPbBr_3$ Perovskite Materials	**Nature of Materials (Endo/Exo.)**	**No. of Endothermic peaks**	**Positions of Endothermic peaks (˚C)**	**ΔH (J/g)**	**ΔC_p (J/g.K)**
Cubic Micro Crystals	Endothermic	5	202.50	5.22	0.76
			255.20	27.38	0.81
			297.60	9.55	1.01
			358.80	265.00	6.14
			610.30	155.10	3.25
Nano Particle	Endothermic	4	204.80	28.62	3.69
			280.70	111.30	4.80
			350.00	349.00	7.41
			593.20	187.70	3.25

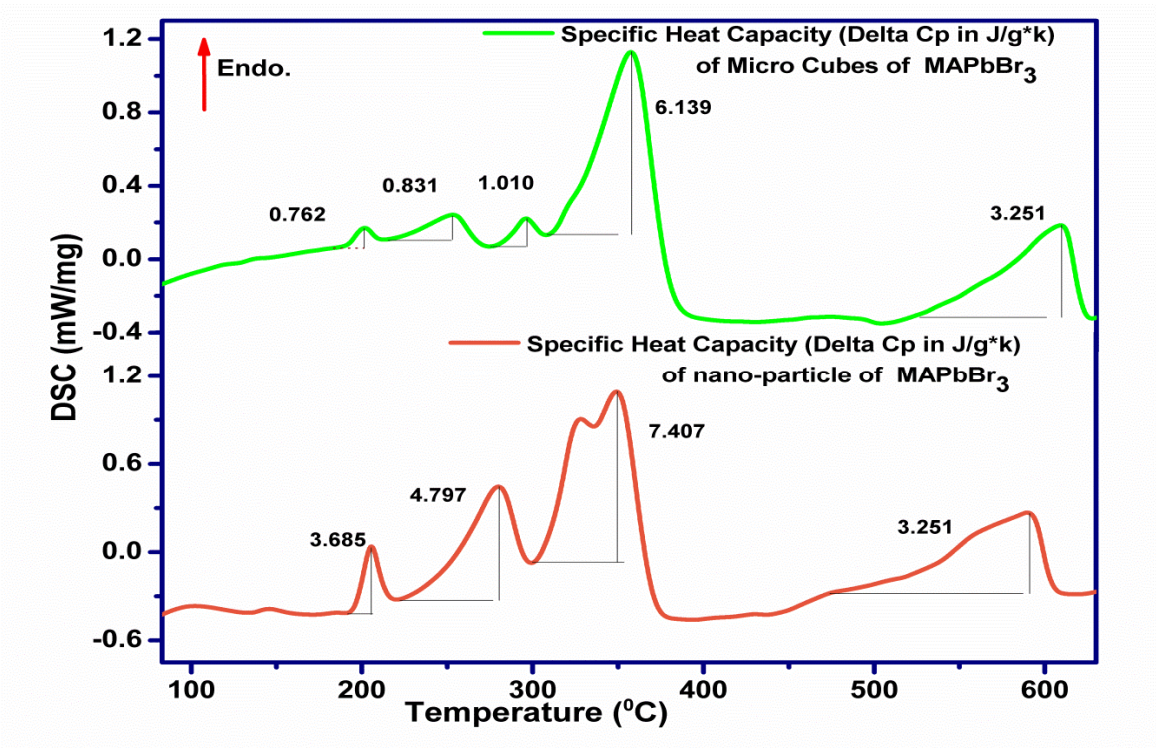

Fig 7: DSC curve with different Specific Heat capacity (ΔC_p) of micro cubes (green line) & (b) nano particle (orange line) of $MAPbBr_3$ perovskite

We have alreadyshowed that nanoparticles display a blue shift due to more surface area and higher energy structure. Nanoparticles have a greater proportion of exposed atoms than bulk particles that increases the surface area of nanomaterials because, by reducing the size of crystals, the number of atoms at the surface of the crystal compared to the number of atoms in the crystal itself increases. This increased surface area increases the enthalpy change and specific heat capacity of the materials which would be stored through an increased vibrational energy[38, 39].Quantitative comparative analysis of enthalpy change and specific heat capacity fordifferent particle size of hybrid perovskite is shown in figure 8 a and b respectively. The value of ΔH and ΔC_p for nanoparticles perovskite are found more than micro crystal perovskite due to enhancement of endothermic peak of nanomaterials. Therefore particlesize of perovskite materials playsa very important role in energy storing devices.

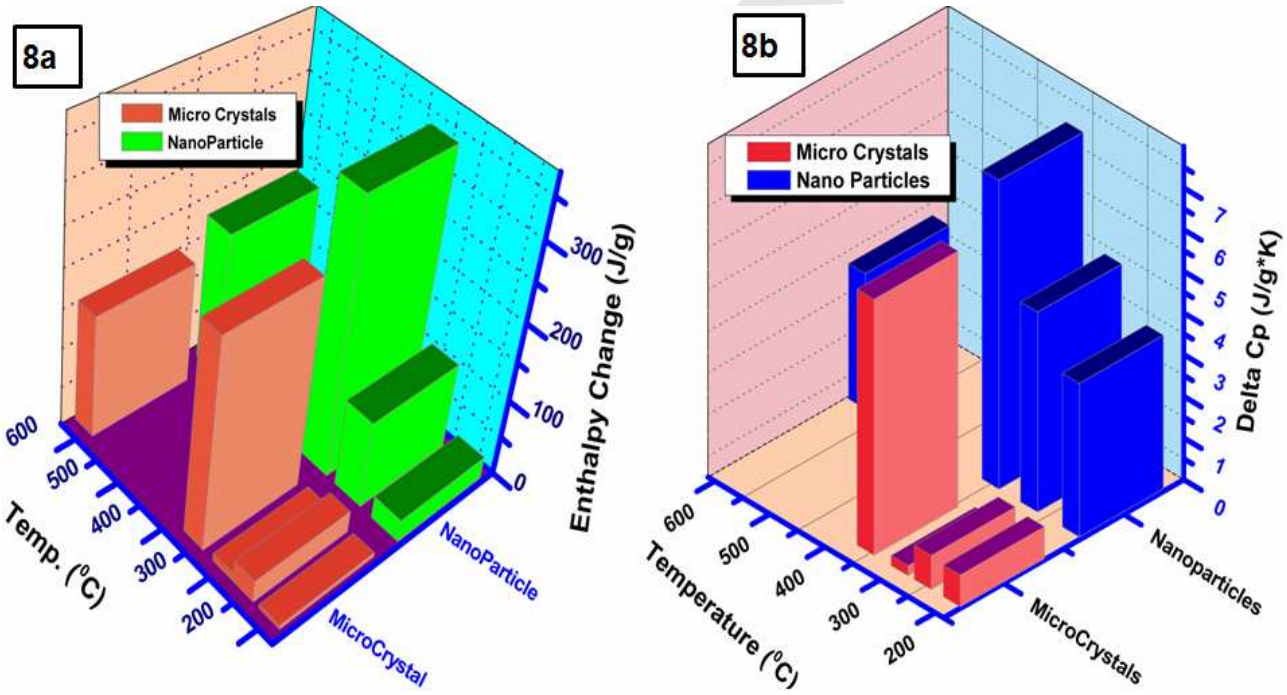

Figure 8: Quantitative analysis of (a) Enthalpy change, ΔH & (b) Specific heat capacity, ΔC_p of micro and nano particles of $MAPbBr_3$ hybrid perovskite

4 CONCLUSION

In this study, we reported here the preparation of MABr and $MAPbBr_3$ perovskite material with cost effective synthesis approach in the ambient conditions without using legands and capping agents. $MAPbBr_3$ has high purity, high crystallinity and cubic phase at ambient condition and room temperature and with decreasing the particle size FWHM peaks increases and intensity of peaks decreases of XRD. Optical properties of materials also have been tuned by tuning the size of the materials (micro-cubes to nano-particles) . This size controlled energy band gap and tunable PL emission of $MAPbBr_3$ perovskite opens up the possibility to develop the low-cost light emitting diodes, photodetectors, stable perovskite solar cells, perovskite batteries, and other energy storing devices. From the thermal analysis (DSC/TG) of the micro-cubes and nano-particles of hybrid perovskite, it is clear that thermal stability and thermal kinetics (enthalpy change and specific heat capacity) of perovskite materials affected by reducing the size of the material. Nanoparticles perovskite has broader endothermic peaks with shifting towards lower melting points than micro-cubes which enhanced the ΔH and ΔCp value of nanomaterials. The thermal reactions occurring in the different halide containing perovskite may be more complicated than usually assumed and that further study is required for a better understanding of the thermodynamic reaction and stability study. In addition, the stability and toxicity due to the presence of lead in organic inorganic halide perovskite is a big issue for commercialization of the type of the materials. So, we need more study regarding stability and lead-free perovskite material.

ACKNOWLEDGEMENT

Rajan acknowledges the National Junior Research Fellowship provided by University Grants Commission (UGC), Govt. of India. Jai Singh would like to acknowledge UGC-India and DST for providing project under UGC Start-up Grant and DST Fast track.

References:

1. Y. Zhang, G. Grancini, Y. Feng, A. M. Asini and M. K. Nazeeruddin, Optimization of Stable Quasi-Cubic $FA_xMA_{1-x}PbI_3$ Perovskite Structure for Solar Cells with Efficiencybeyond 20%, ACS Energy Lett. 2(4)(2017) 802-806.
2. T. Singh, J. Singh and T. Miyasaka, Role of Metal Oxide Electron-Transport Layer Modification on the Stability of High Performing Perovskite Solar Cells, ChemSusChem 9 (2016) 1-9.
3. R. Sheng,M. T. Hörantner,Z. Wang,Y. Jiang,W. Zhang, A. Agosti,S. Huang,X. Hao,A. Ho-Baillie,M. Green,and H. J. Snaith, Monolithic Wide Band Gap Perovskite/Perovskite Tandem Solar Cells with Organic Recombination Layers, J. Phys. Chem. C 121 (2017) 27256−27262.
4. S. Demchyshyn, J. M. Roemer, H. Groiß, H. Heilbrunner, C. Ulbricht, D. Apaydin, A. Böhm, U. Rütt, F. Bertram, G. Hesser, M. C. Scharber, N. S. Sariciftci, B. Nickel, S. Bauer, E. D. Głowacki, M. Kaltenbrunner, Confining metal-halide perovskites in nano porous thin films, Sci. Adv. 3 (2017) e1700738.
5. B. Wenger, P. K. Nayak, X. Wen, S. V. Kesava, N. K. Noel & H. J. Snaith, Consolidation of the optoelectronic properties of $CH_3NH_3PbBr_3$ perovskite single crystals, Nat. Commun. 8(1) (2017) 590.
6. Y. Zhao and K. Zhu, Organic–inorganic hybrid lead halide perovskites for optoelectronic and electronic applications, Chem. Soc. Rev. 45 (2016) 655.
7. S. A. Veldhuis, P. P. Boix, N. Yantara, M. Li, T. C. Sum, N. Mathews & G. Mhaisalkar, Perovskite Materials for Light-Emitting Diodes and Lasers, Adv. Mater. 28 (2016) 6804-6834.
8. X. Tan, B. Zhang, and G. Zou, Electrochemistry and Electrochemiluminescence of Organometal Halide Perovskite Nanocrystals in Aqueous Medium, J. Am. Chem. Soc. 139 (2017) 8772−8776.
9. Y. Gao, S. Wang, C. Huang, N. Yi, K. Wang, S. Xiao & Q. Song, Room temperature three-photon pumped $CH_3NH_3PbBr_3$ perovskite microlasers, Sci Rep. 7 (2017) 45391.

10. A. Kojima K.Teshima, Y. Shirai, T. Miyasaka, Organometal halide perovskite as visible light sensitizers for photovoltaic cells, J. Am. Chem. Soc. 131 (2009) 6050.
11. T. Singh, Y. Udagawa, M. Ikegami, H. Kunugita,K. Ema, and T. Miyasaka, Tuning of perovskite solar cell performancevia low-temperature brookite scaffoldssurface modifications, APL Materials 5, (2017) 016103.
12. R. J. Sutton, G. E. Eperon, L. Miranda, E. S. Parrott, B. A. Kamino, J. B. Patel, M. T Hörantner, M. B. Johnston, A. A. Haghighirad, D. T Moore, H. J. Snaith, Bandgap□tunable cesium lead halide perovskites with high thermal stability for efficient solar cells, 6 (2016) 1502458.
13. H. Rao, W. Sun, S. Yen, W. Yan, Y. Li, H. Peng, Z. Liu, Z. Bin, C. Huang, Solution-Processed CuS NPs as an Inorganic Hole-Selective Contact Material for Inverted Planar Perovskite Solar Cells ACS Appl. Mater. Interfaces 8 (2016) 7800-7805.
14. Y. Liu, L. A. Renna, M. Bag, Z. A. Page, P. Kim, J. Choi, T. Emrick, D. Venkataraman, and T. P. Russell, High Efficiency Tandem Thin-Perovskite/Polymer Solar Cells with a Graded Recombination Layer,ACS Appl. Mater. Interfaces 8 (2016) 7070-7076.
15. T. Singh and T. Miyasaka, Stabilizing the Efficiency Beyond 20% with a Mixed CationPerovskite Solar Cell Fabricated in Ambient Air under Controlled HumidityAdv. Energy Mater. 2017, 1700677, DOI: 10.1002/aenm.201700677A.
16. NREL chart, http://www.nrel.gov/ncpv/images/efficiency_chart.jpg (accessed: December, 2017).
17. A. Poglitsch and D. Weber, Disorder in Methylammonium trihalogen oplumbates (II) Observed by Millimeter-wave Spectroscopy, J. Chem. Phys. 87 (1987) 6373–6378.
18. B. Suarez, , V. Gonzalez-Pedro, T. S. Ripolles, R. S.Sanchez, L. Otero and I. Mora-Sero,Recombination Study of Combined Halides (Cl, Br, I) Perovskite Solar Cells, J. Phys.Chem. Lett. 5 (2014) 1628–1635.

19. S. Mali, C. S. S,him and C. K. Hong, Highly stable and efficient solid-state solar cells based on methylammonium lead bromide ($CH_3NH_3PbBr_3$) perovskite quantum dots,NPG Asia Materials 7 (2015) e208.

20. D. M. Jang, K. Park, , D. H. Kim, J. Park, F. Shojaei, J. Lee, Reversible Halide Exchange Reaction of Organometal Trihalide Perovskite Colloidal Nanocrystals for Full-Range Band Gap Tuning, Nano Letter,15 (8) (2015) 5191–5199.

21. W. J. Yin, J. H. Yang, J. Kang, Y. Yan, S. H. Wei,Reversible Halide Exchange Reaction of Organometal Trihalide Perovskite Colloidal Nanocrystal for Full-Range Band Gap Tuning,J. Mater Chem. A3 (2015) 8926-8942.

22. S. Gonalez, R. E. Galian, J. Perez-Prieto, maximizing the emissive properties of $CH_3NH_3PbBr_3$ perovskite nanoparticles, J. Mater. Chem. A 3 (2015) 9187-9193.

23. Y. Zhou, T. Zhang, C. Li., Z. Liang, L. Gong, J. Chen, W. Xie, J. Xie, P. Liu, Rapid growth of high quality perovskite crystal by solvent mixing,CrystEngComm.18 (2016) 1184-1189.

24. Y. Liu, Z. Yang, D. Cui, X. Ren, J. Sun, X. Liu, J. Zhang, Q. Wei, H. Fan, F. Yu, X. Zhang, C. Zhao, S. Liu,Two-Inch-Sized Perovskite CH3NH3PbX3 (X = Cl, Br, I) Crystals: Growth and Characterization, Adv Mater. 27 (2015) 5176-5183.

25. R. K. Singh, R. Kumar, J. Singh, Effect of precursor ratio on crystallanity and thermal stability of $CH_3NH_3PbI_3$, AIP Conference Proceeding 1832 (2017) 050056.

26. J. S. Manser, J. A. Cristians, P. V. Kamat, Intriguing Optoelectronic Properties of Metal Halide Perovskites, Chem. Rev. 116 (21) (2016) 12956-13008.

27. D. Priante, I. Dursun, M. S. Alias, D. Shi, V. A. Melnikov, T. K. Ng, O. F. Mohammed, O. M .Bakr, B. S. Ooi, The recombination mechanisms leading to amplified spontaneous emission at the true-green wavelength in $CH_3NH_3PbBr_3$ perovskites, Appled Physics Letters 106(2015) 081902.

28. G. K. Willamson, W. H. Hall, X-ray line broadening from filed aluminium and wolfram Die verbreiterung der roentgeninterferenzlinien von aluminium- und wolframspaenen A.cta Mettall. 1(1953) 22.

29. L. C. Schmidt, A. Petegas, S. G. Carrero, O. Malinkiewicz, S. Agoura, G. M. Espallargas, H. J. Bolink, R. E. Galian, J. Perez-Prieto, Nontemplate synthesis of $CH_3NH_3PbBr_3$ perovskite nanoparticles, J. Am. Chem. Soc. 136 (2014) 850-853.

30. A. Kojima, M. Ikegami, K. Teshima, T. Miyasaka, Highly Luminescent Lead Bromide Perovskite Nanoparticles Synthesized with Porous Alumina Media, Chem. Let. 41 (2012) 397-399.

31. S. Mireshadi, S. Ahmadi—Kandjani, Efficient thin luminescent solar concentrator based on Organometal halide perovskite, Dye and Pigments 26 (2015) 15-21.

32. P. Kumar, C. Moth, V. C. Nair and K. S. Narayan,Quantum Confinement Effects in Organic Lead Tribromide Perovskite Nanoparticles, J. Phys. Chem. C, 120 (2016) 18333-18339.

33. Y. Yamada, T. Nakamura, T. Nakamura, M. Endo, A. Wakamiya, Y. Kanemitsu, Photo carrier Recombination Dynamics in Perovskite $CH_3NH_3PbI_3$ for Solar Cell Applications,J. Am. Chem. Soc.136(2014) 11610-11613.

34. H. R. Xia, W. T. Sun, L. M. Peng, Hydrothermal synthesis of Organometal halide perovskites for Li-ion batteries, Chem. Commun. 51 (2015) 13787-13790.

35. M. F. Aygler, M. D. Weber, B. M. D. Puscher, D. D. Medina, P. Docampo, R. D. Costa, , Light-Emitting Electrochemical Cells Based on Hybrid Lead Halide Perovskite Nanoparticles, J. Phys. Chem. C 119 (2015) 12047.

36. R. K. Singh, N. Jain, J. Singh, R. Kumar, Stability behaviour of chemically synthesized organic electrolyte salts and Methylammonium lead halide perovskite light harvester, Advanced Materials Letters 8 (6) (2017) 707-711.

37. E. Martine, The effect of particle size on the thermal properties of serpentine minerals, The American Mineralogist 46 (1961) 901-912.

38. L. Wang, Z. Tan, S. Meng, D. Liang, G. Li, Enhancement of molar heat capacity of nanostructured Al2O3. J. Nanoparticle Res. 3 (2001) 483-487.

39. B. X. Wang, L. P. Zhou, X. F. Peng,Surface and Size Effects on the Specific Heat Capacity of Nanoparticles, International Journal of Thermophysics 27 (1) (2006) 139-151.

Highlights:

- Solution processed methyl ammonium lead bromide was highly cubic crystalline at room temperature.
- $MAPbBr_3$, micro-cubes was more thermally stable than nano-particles.
- High absorbance and luminescence property show the light harvesting nature of the materials.
- Change in enthalpy and specific heat capacity of perovskite particle was increased by reducing the particle size.